

Structural, morphological, electrical and dielectric properties of $\text{Ni}_{1.1}\text{Zr}_{0.1}\text{Fe}_{1.8}\text{O}_4$ Nanoparticles

Tukaram S. Saraf*, N. R. Shamkuwar

Department of Physics, Dr. Babasaheb Ambedkar Marathwada University, Aurangabad (M.S.), 431001, India.

Abstract

In the present work, the structural, morphological, electrical and dielectric properties of $\text{Ni}_{1.1}\text{Zr}_{0.1}\text{Fe}_{1.8}\text{O}_4$ ferrite nanoparticles were studied before and after Nd: YAG laser irradiation. The synthesized samples of ferrite nanoparticles were prepared by sol-gel auto combustion technique using AR grade chemicals of 99% purity. The prepared sample was characterized by X-ray diffraction technique. The X-ray diffraction pattern revealed that prepared sample having single phase cubic spinel structure. Crystal defects produced in the spinel lattice were studied before and after Nd: YAG laser irradiation in order to report the changes in structural properties of the Ni-Zr ferrite nanoparticles. The average crystallite size (t), lattice parameter (a) and other structural parameters of laser-irradiated and un-irradiated Ni-Zr spinel ferrite system was calculated from XRD data. The morphological studies were carried out using scanning electron microscopy (SEM). Using SEM images grain size and specific surface area were calculated. The temperature dependence of D.C. electrical resistivity of irradiated and unirradiated sample was carried out using two probe technique. Semiconducting nature of the sample was confirmed from Arrhenius plot. The frequency dependence of dielectric constant (ϵ'') and dielectric loss tangent ($\tan \delta$) were studied using LCR-Q meter at room temperature.

Keywords: Nd: YAG laser, Ni-Zr nanoparticles, XRD, dielectric.

1. Introduction

In the recent years, nanosize spinel ferrite particles received a considerable attention because of their interesting structural and magnetic properties [1, 2]. It is found that when the particle diameter reduce to nanometer dimension spinel ferrite particles may exhibit super paramagnetic behaviour, which is of great interest from the point of view of their applications [3]. Spinel ferrites are compounds of iron oxides and some metal oxides and they exhibits important electrical and magnetic properties, which made them extensively useful in technological and industrial applications such as magnetic storage in microwave devices etc[4]. Nickel ferrite is one of the important ferrites used for different technological applications [5]. It crystallizes in inverse spinel structure i.e. tetrahedral sites are occupied by ferric ions and the octahedral sites by ferric and nickel ions.

During the last two decades, several investigations have deals with the influence of gamma, neutron and swift heavy ion irradiation on the physical properties of spinel ferrites [6-8]. It is known that high-energy photons interact with solid by exciting electrons from one of the filled bands into the unbound continuum levels above the conduction band. Recently, it has reported the effect of gamma and laser irradiation on cation distribution, structural and magnetic, morphological, electric and dielectric properties of spinel ferrite [9-11].

In recent research work, the effect of ionizing radiations on properties of nanostructures materials has gained much attention, especially with laser irradiation and opened new era in optimizing the properties of laser irradiated materials to be more applicable from the viewpoint of theory and applications. Several workers have studied the effect of gamma irradiation and modifications in the properties of bulk and nanoparticles of ferrites [12-14] but no investigations are available in the literature which shows the effect of laser irradiation on properties of $\text{Ni}_{1.1}\text{Zr}_{0.1}\text{Fe}_{1.8}\text{O}_4$ nanoparticles.

However, to our knowledge reports on zirconium substituted in nickel ferrite are . Zirconium is a lustrous, grayish-white, soft, ductile and malleable metal which is solid at room temperature, though it becomes hard and brittle at lower purities. Zirconium is highly resistant to corrosion by alkalis, acids, salt water and other agents.

In order to investigate the effects appearing under influence of laser irradiation this may be technologically important in the ferrites with spinel structure. The present investigation is focused on effect of laser irradiation on structural, morphological, electrical and dielectric properties of $\text{Ni}_{1.1}\text{Zr}_{0.1}\text{Fe}_{1.8}\text{O}_4$ synthesized by sol-gel auto combustion technique.

2. Experimental

Nanoparticles of Ni-Zr spinel ferrite were prepared by sol-gel auto-combustion technique by using the nitrates of respective cations and citric acid as a fuel. The metal

nitrates to citric acid ratio was taken as 1:3. The metal nitrate solutions were mixed in the required stoichiometric ratios in distilled water. The final pH of the solution was maintained at 7 by using ammonia solution. The solution mixture was slowly heated around 90 °C with constant stirring to obtain nanoparticles of $\text{Ni}_{1.1}\text{Zr}_{0.1}\text{Fe}_{1.8}\text{O}_4$. In order to remove impurity and form crystallinity the as-prepared samples of $\text{Ni}_{1.1}\text{Zr}_{0.1}\text{Fe}_{1.8}\text{O}_4$ spinel ferrite was sintered at 700 °C for 4 h. The sintered nano-powders were pressed in pellet form of 10 mm diameter and 3 mm thickness and treated as the precursor for laser irradiation. The prepared sample was characterized by standard techniques such as X-ray diffraction, Scanning electron microscopy and for electrical as well as dielectric measurements.

Characterizations

The pellets of Ni–Zr synthesized material was irradiated with flash lamp pumped Nd: YAG laser and it was operated in the free running mode with the pulse width of 200 μs and a spot diameter of 8 mm ($1/e^2$ points—the diameter of the beam where the intensity falls $1/e^2$ times the peak intensity of the beam). X-ray diffraction (XRD) patterns of the $\text{Ni}_{1.1}\text{Zr}_{0.1}\text{Fe}_{1.8}\text{O}_4$ spinel ferrite samples before and after laser irradiation were recorded on a Miniflex–II X-ray diffractometer with Cu–K α radiation ($\lambda = 1.5405 \text{ \AA}$). The microstructure studies were carried out using Scanning electron microscopy (SEM). Using SEM images grain size and specific surface area were calculated. The temperature dependence of D.C. electrical resistivity of all the irradiated and unirradiated samples were carried out on disc shaped pellets of 10 mm diameter and about 3 mm thickness using two probe technique and in the temperature range 450K to 750K with step of 10 K. The electrical resistivity was estimated by measuring the resistance ‘R’ of the samples. The frequency dependence of dielectric constant (ϵ'') and dielectric loss tangent ($\tan \delta$) in the range from 20 Hz – 1 MHz were studied using a precision LCR–Q meter bridge (Model HP 4284 A) at room temperature.

3. Results and Discussions

X-ray diffraction

The room temperature XRD patterns of un-irradiated and laser irradiated $\text{Ni}_{1.1}\text{Zr}_{0.1}\text{Fe}_{1.8}\text{O}_4$ ferrite nanoparticles are shown in Fig 1.

All the X-ray diffraction patterns show the reflections (220), (311), (222), (400), (422), (511), (440). The analysis of X-ray diffraction patterns indicates that the samples exhibit single phase cubic spinel structure.

A careful examination of the XRD patterns reveals that the intensity of the Ni–Zr nanoparticles is decreases after

the irradiation by Nd: YAG laser. It is noted from XRD patterns that there is a shift in reflections towards lower 2θ side. Using X-ray diffraction data the lattice constant was calculated for unirradiated and irradiated of sample by using standard relation [15].

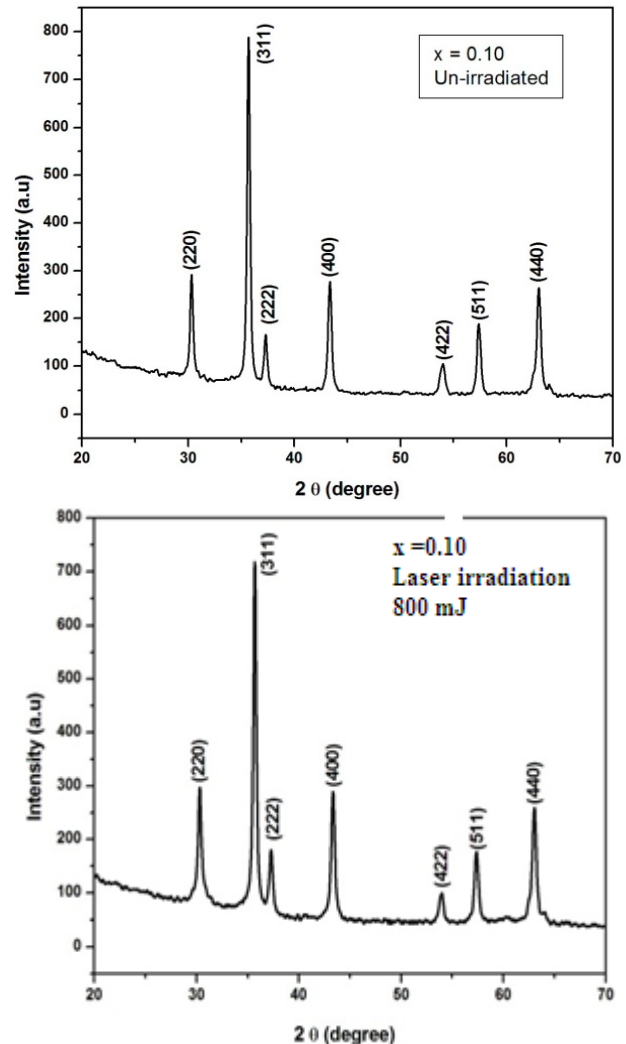


Fig. 2. XRD pattern of Un-irradiated and laser irradiated $\text{Ni}_{1.1}\text{Zr}_{0.1}\text{Fe}_{1.8}\text{O}_4$ nanoparticles

The values of lattice constant are given in Table 1. From the table 1 it can be seen that the lattice constant increases after laser irradiation on the Ni–Zr ferrite nanoparticles.

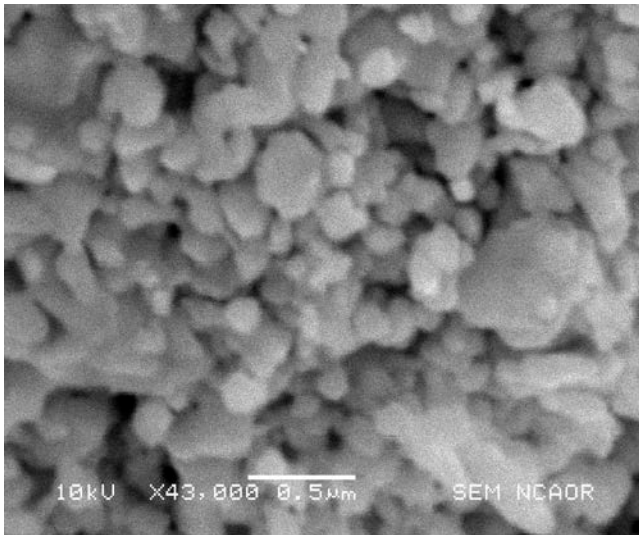
Table.1 Lattice constant ‘a’ (\AA) and crystallite size ‘t’ (nm) of unirradiated and laser irradiated $\text{Ni}_{1.1}\text{Zr}_{0.1}\text{Fe}_{1.8}\text{O}_4$ nanoparticles

Sample	a (Å)	t nm
Un-irradiated	8.3318	39
Nd:YAG laser Irradiated	8.3426	32

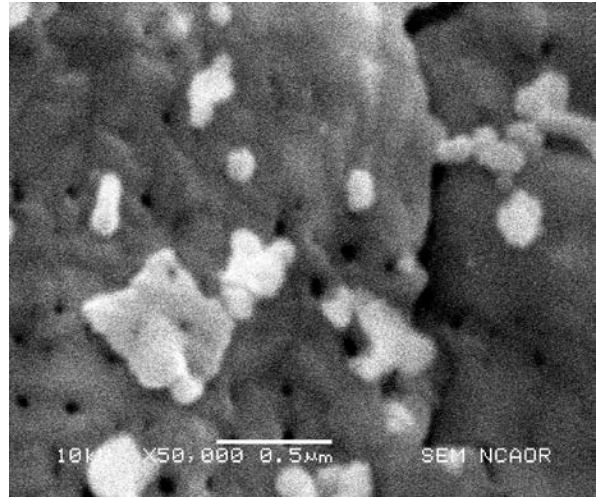
The crystallite size of all the Ni-Zr nanoparticles was determined by using well known Scherrer's equation [16]. The most intense peak (311) of the XRD pattern was used to determine the crystallite size. The values of crystallite size are represented in Table 1. The crystallite size values are found to be 39 and 32 nm. It can be also understood that after laser irradiation the crystallite size is decreases.

Scanning Electron Microscope Study

Fig. 2 shows morphological pattern of the $Ni_{1.1}Zr_{0.1}Fe_{1.8}O_4$ spinel ferrite nanoparticles taken by scanning electron microscope (SEM). Evidently, from SEM images of the sintered zirconium substituted nickel spinel ferrite samples it was seen that the morphology of the particles were almost spherical in shape, but agglomerated to some extent due to the interaction between magnetic nanoparticles. The formation of nano size crystallites was confirmed through SEM images. The grain size was determined by linear intercept method estimated using standard relation [17].



(a)



(b)

Fig. 2 SEM images for (a) un-irradiation and (b) Nd: YAG laser irradiation $Ni_{1.1}Zr_{0.1}Fe_{1.8}O_4$ nanoparticles

The average grain size calculated from linear intercept method was found to be in nanometer range i.e. 75 nm and 78 nm for unirradiated and Nd:YAG laser irradiated samples respectively. The specific surface area of unirradiated and Nd:YAG laser irradiated samples using SEM images was calculated according to the relation [18] and the values are 14.64 and 14.09 m²/g for unirradiated and Nd:YAG laser irradiated samples respectively. Since the particle size decreases the surface area increases which indicate the nanocrystalline nature of the samples. It is well known that the crystallite size and surface area play an important role on the properties of ferrites.

D. C. Resistivity

Figure 3 shows the variation of resistivity (log ρ) against reciprocal of temperature (1000/T) for unirradiated and irradiated $Ni_{1.1}Zr_{0.1}Fe_{1.8}O_4$ spinel ferrite. Resistivity decreases continuously with the increasing temperature, revealing the semiconducting nature of the prepared samples [19]. The plot is divided into two distinct regions corresponding to the ferrimagnetic and paramagnetic region. The slope is observed to change at a particular temperature and this temperature corresponds to the Curie temperature of the sample. The similar behaviour of resistivity as a function of temperature is reported for other spinel ferrite nanoparticle [7, 20, 21]. The distortion in the crystal after Nd:YAG laser irradiation causes increase in resistivity.

Activation Energy

The activation energy was calculated from the slop of Arrhenius plot and the values are attributed in the table 2. Since the resistivity has been found to increase after

irradiation, a rise in activation energy is expected. Our results are in good agreement with that reported in the literature [22].

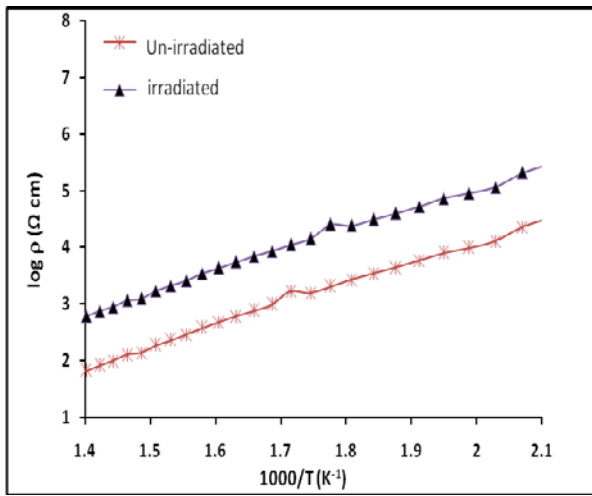


Fig. 3. Variation of DC electrical resistivity with reciprocal of temperature for Un-irradiation $Ni_{1.1}Zr_{0.1}Fe_{1.8}O_4$ nanoparticles

Table 2 Activation energy in paramagnetic region (E_p) and ferrimagnetic region (E_f) for Un-irradiated and irradiated $Ni_{1.1}Zr_{0.1}Fe_{1.8}O_4$ nanoparticles

Sample	E_p (eV)	E_f (eV)	ΔE (eV)
Un-irradiated	0.9327	0.5343	0.3984
Nd:YAG laser Irradiated	0.715	0.352	0.363

Dielectric Properties

The dielectric behavior of $Ni_{1.1}Zr_{0.1}Fe_{1.8}O_4$ as a function of frequency was studied in the form of dielectric constant and dielectric loss tangent also the effect of 112 mJ Nd: YAG laser irradiation on it.

The variation of dielectric constant and loss determined in the frequency range of 100 Hz to 1 MHz at room temperature for $Ni_{1.1}Zr_{0.1}Fe_{1.8}O_4$ before and after irradiation is shown in figure 4 (a, b). The dielectric constant decreases with increase in frequency for the compositions showing the dielectric behavior as reported earlier in the literature [23] also similar behavior is observed for 112 mJ Nd:YAG laser irradiated samples. The rapid decrease at low frequencies of dielectric

constant was observed while at high frequencies it is almost constant for both before and after irradiation.

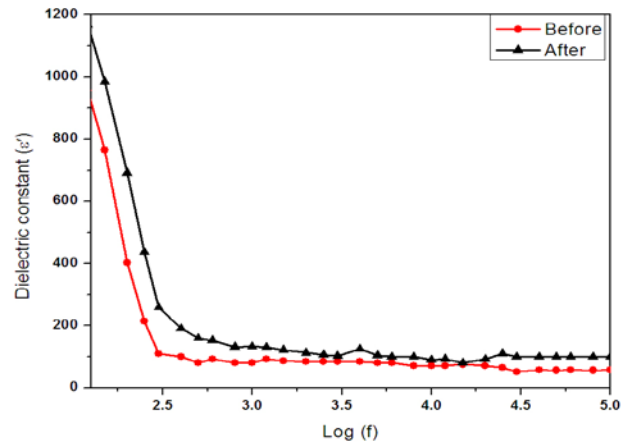


Fig. 4 (a) Variation of the dielectric constant with frequency log (f) for un-irradiation and (1200 mJ dose rate) Nd: YAG laser irradiation

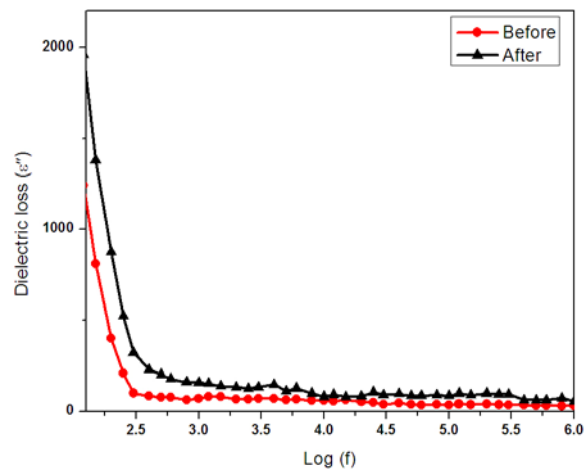


Fig. 4 (b) Variation of the dielectric loss (ϵ'') with frequency log (f) for un-irradiation and (1200 mJ dose rate) Nd: YAG laser irradiation

The rapid change in dielectric constant at low frequencies can be attributed to the polarization of the cations due to the change in valence state. On the other hand at higher frequencies it is almost constant because of the inability to follow the applied external electric field. Usually the dielectric constant as function of frequency is explained on the basis of Maxwell–Wagner interfacial polarization model and the Koop’s theory [24]. The Maxwell–Wagner interfacial polarization model depends on the heterogeneous structure which usually consists of the grains and the poor conducting grain boundaries. Also it comprises of the space charge polarization which is governed by the available number of space charge carriers.

It can be assumed that the mechanism of interfacial dielectric polarization is similar to the hopping mechanism of electrons. It is a well known and established fact that the dielectric constant and conduction mechanism have a strong correlation [25, 26], where the dielectric behavior has explained on the basis of available Fe^{2+} ions between electronic exchange like $\text{Fe}^{3+} \leftrightarrow \text{Fe}^{2+}$. It results in a local displacement of electrons in the direction of applied external electric field which determines the polarization and hence the dielectric constant of spinel ferrites. Under applied electric field, according to hopping mechanism the electrons reach to the insulating grain boundaries and accumulate there resulting increase in interfacial polarization hence the dielectric constant at lower frequencies is high. With the increase in frequency the interfacial polarization decreases and attains the constant value because the polarization of induced moments could not follow the applied electric field. Also the electronic exchange between $\text{Fe}^{3+} \leftrightarrow \text{Fe}^{2+}$ lags behind the applied frequency. Hence, the dielectric constant at high frequencies is almost constant. The lower values of dielectric constant at high frequency are in close agreement with that of reported earlier in the literature [27, 28] for nanocrystalline spinel ferrites.

The variation in dielectric loss tangent as a function of frequency of $\text{Ni}_{1.1}\text{Zr}_{0.1}\text{Fe}_{1.8}\text{O}_4$ sample determined in 100Hz to 1MHz frequency range at room temperature also for irradiated $\text{Ni}_{1.1}\text{Zr}_{0.1}\text{Fe}_{1.8}\text{O}_4$ and this are depicted in figure 4 (c).

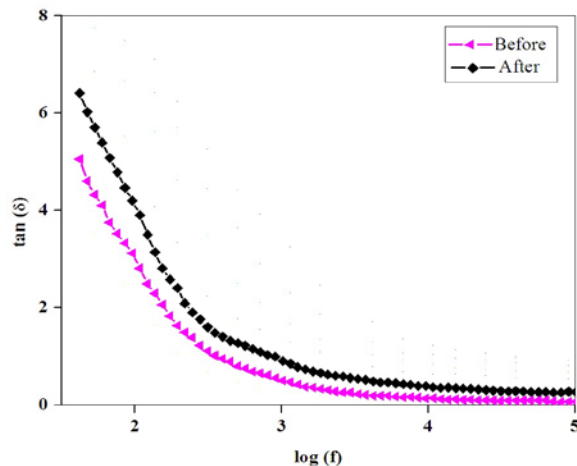


Fig. 4 (c) Variation of the tangent loss ($\tan\delta$) with frequency $\log(f)$ for un-irradiation and (1200 mJ dose rate) Nd: YAG laser irradiation $\text{Ni}_{1.1}\text{Zr}_{0.1}\text{Fe}_{1.8}\text{O}_4$ nanoparticles

It is seen that the dielectric loss tangent decreases with increase in frequency for $\text{Ni}_{1.1}\text{Zr}_{0.1}\text{Fe}_{1.8}\text{O}_4$ ferrite before

and after irradiation, at low frequency the dielectric loss tangent decreases rapidly and becomes almost constant at high frequency. The decreases in dielectric constant with frequency can be attributed to the fact that the hopping frequency of charge carriers can not follow the applied electric field. When the hopping frequency of charge carriers equal with the applied frequency of electric field, the maximum energy is transferred to the oscillating ions and the peaks observed which results in to the power loss. The similar behavior of the dielectric loss was observed in literature [29].

4. Conclusion

Nickel zirconium spinel ferrite nanoparticles were successfully synthesized by sol gel auto combustion method. The X-ray diffraction pattern of the prepared sample showed that before and after laser irradiation is in single phase and cubic spinel structure. The structural parameters of prepared nanoparticles have been influenced after laser irradiation. Also the morphology of present sample is affected after irradiation. The increase in DC resistivity was observed after Nd:YAG laser irradiation and the dielectric properties also influenced.

Acknowledgement: The author Tukaram S. Saraf is thankful to Raja Ramanna Centre for Advanced Technology for providing laser radiation facility and Prof. K. M. Jadhav, Prof and ex-head, Dept. of Physics, Dr. Babasaheb Ambedkar Marathwada University, Aurangabad for his time to time guidance.

References

- [1] K. Jalaiah, K.V. Babu, Structural, magnetic and electrical properties of nickel doped Mn-Zn spinel ferrite synthesized by sol-gel method, *Journal of Magnetism and Magnetic Materials*, 423 (2017) 275-280.
- [2] R. Pawar, S. Desai, S. Patange, S. Jadhav, K. Jadhav, Interatomic bonding and dielectric polarization in Gd 3+ incorporated Co-Zn ferrite nanoparticles, *Physica B: Condensed Matter*, (2017).
- [3] M. Foresti, A. Vázquez, B. Boury, Applications of bacterial cellulose as precursor of carbon and composites with metal oxide, metal sulfide and metal nanoparticles: A review of recent advances, *Carbohydrate Polymers*, 157 (2017) 447-467.
- [4] M.N. Akhtar, M.A. Khan, M. Ahmad, M. Nazir, M. Imran, A. Ali, A. Sattar, G. Murtaza, Evaluation of structural, morphological and magnetic properties of $\text{CuZnNi}(\text{Cu}_x\text{Zn}_{0.5-x}\text{Ni}_{0.5}\text{Fe}_2\text{O}_4)$ nanocrystalline ferrites for core, switching and MLCI's applications, *Journal of Magnetism and Magnetic Materials*, 421 (2017) 260-268.
- [5] T. Ruthradevi, J. Akbar, G.S. Kumar, A. Thamizhavel, G. Kumar, R. Vatsa, G. Dannangoda, K. Martirosyan, E. Girija, Investigations on nickel ferrite embedded calcium phosphate

- nanoparticles for biomedical applications, *Journal of Alloys and Compounds*, 695 (2017) 3211-3219.
- [6] V.J. Angadi, A. Anupama, H.K. Choudhary, R. Kumar, H. Somashekarappa, M. Mallappa, B. Rudraswamy, B. Sahoo, Mechanism of γ -irradiation induced phase transformations in nanocrystalline Mn 0.5 Zn 0.5 Fe 2 O 4 ceramics, *Journal of Solid State Chemistry*, 246 (2017) 119-124.
- [7] A.V. Raut, S. Jadhav, D. Shengule, K. Jadhav, Structural and magnetic characterization of 100-kGy Co60 γ -ray-irradiated ZnFe2O4 NPs by XRD, W–H plot and ESR, *Journal of Sol-Gel Science and Technology*, 79 (2016) 1-11.
- [8] N. Imam, A. Hashhash, Photoluminescence of γ -irradiation induced distortion on Ga based ferrosipinel material to be used as γ -rays detector, *Nuclear Instruments and Methods in Physics Research Section A: Accelerators, Spectrometers, Detectors and Associated Equipment*, 767 (2014) 353-358.
- [9] A. Jagadisha, E.N.H. Jayanna, N. Desai, Effect of Gamma Radiation on Magnetic Properties of Magnesium Zinc Ferrite, *International Journal of Innovative Research and Development* | ISSN 2278–0211, 5 (2016).
- [10] H. Hassan, T. Sharshar, M. Hessien, O. Hemeda, Effect of γ -rays irradiation on Mn–Ni ferrites: Structure, magnetic properties and positron annihilation studies, *Nuclear Instruments and Methods in Physics Research Section B: Beam Interactions with Materials and Atoms*, 304 (2013) 72-79.
- [11] M.L. Mane, V. Dhage, S.E. Shirsath, R. Sundar, K. Ranganathan, S. Oak, K. Jadhav, Nd: YAG laser irradiation effects on the structural and magnetic properties of polycrystalline cobalt ferrite, *Journal of Molecular Structure*, 1035 (2013) 27-30.
- [12] R. Panda, K. Routray, D. Behera, Effect of Gamma Irradiation on Structural and Magnetic Properties of Bi Substituted Cobalt Ferrite Nanoparticles, (2016).
- [13] A.V. Raut, D. Kurmude, D. Shengule, K. Jadhav, Effect of gamma irradiation on the structural and magnetic properties of Co–Zn spinel ferrite nanoparticles, *Materials Research Bulletin*, 63 (2015) 123-128.
- [14] P. Naik, R. Tangsali, S. Meena, P. Bhatt, B. Sonaye, S. Sugur, Gamma radiation roused lattice contraction effects investigated by Mössbauer spectroscopy in nanoparticle Mn–Zn ferrite, *Radiation Physics and Chemistry*, 102 (2014) 147-152.
- [15] W.M. Haynes, *CRC handbook of chemistry and physics*, CRC press, 2014.
- [16] A.C. Nawle, A.V. Humbe, M. Babrekar, S. Deshmukh, K. Jadhav, Deposition, characterization, magnetic and optical properties of Zn doped CuFe 2 O 4 thin films, *Journal of Alloys and Compounds*, 695 (2017) 1573-1582.
- [17] P.J. Schoeneberger, *Field book for describing and sampling soils*, Government Printing Office, 1998.
- [18] U. Åkesson, J. Lindqvist, M. Göransson, J. Stigh, Relationship between texture and mechanical properties of granites, central Sweden, by use of image-analysing techniques, *Bulletin of Engineering Geology and the Environment*, 60 (2001) 277-284.
- [19] A. Jayaraman, V. Narayanamurti, E. Bucher, R. Maines, Continuous and discontinuous semiconductor-metal transition in samarium monochalcogenides under pressure, *Physical Review Letters*, 25 (1970) 1430.
- [20] R. Alange, P.P. Khirade, S.D. Birajdar, K. Jadhav, Influence of Al–Cr co-substitution on physical properties of strontium hexaferrite nanoparticles synthesized by sol–gel auto combustion method, *Journal of Materials Science: Materials in Electronics*, 28 (2017) 407-417.
- [21] B. Devmunde, A. Raut, S. Birajdar, S. Shukla, D. Shengule, K. Jadhav, Structural, Electrical, Dielectric, and Magnetic Properties of Cd2, *Journal of Nanoparticles*, 2016 (2016).
- [22] A. Raut, D. Kurmude, S. Jadhav, D. Shengule, K. Jadhav, Effect of 100 kGy γ -irradiation on the structural, electrical and magnetic properties of CoFe 2 O 4 NPs, *Journal of Alloys and Compounds*, 676 (2016) 326-336.
- [23] M. Subramanian, D. Li, N. Duan, B. Reisner, A. Sleight, High dielectric constant in ACu 3 Ti 4 O 12 and ACu 3 Ti 3 FeO 12 phases, *Journal of Solid State Chemistry*, 151 (2000) 323-325.
- [24] M. George, S.S. Nair, K. Malini, P. Joy, M. Anantharaman, Finite size effects on the electrical properties of sol–gel synthesized CoFe2O4 powders: deviation from Maxwell–Wagner theory and evidence of surface polarization effects, *Journal of Physics D: Applied Physics*, 40 (2007) 1593.
- [25] G.R. Mohan, D. Ravinder, A.R. Reddy, B. Boyanov, Dielectric properties of polycrystalline mixed nickel–zinc ferrites, *Materials Letters*, 40 (1999) 39-45.
- [26] L.G. Van Uitert, Dielectric properties of and conductivity in ferrites, *Proceedings of the IRE*, 44 (1956) 1294-1303.
- [27] D. Ferry, High-field transport in wide-band-gap semiconductors, *Physical Review B*, 12 (1975) 2361.
- [28] J.F. Johnson, R. Cole, Dielectric polarization of liquid and solid formic acid1, *Journal of the American Chemical Society*, 73 (1951) 4536-4540.
- [29] K. Verma, A. Kumar, D. Varshney, Effect of Zn and Mg doping on structural, dielectric and magnetic properties of tetragonal CuFe 2 O 4, *Current Applied Physics*, 13 (2013) 467-473.